

Bias controlled capacitive driven cantilever oscillation for high resolution dynamic force microscopy

Jinjin Zhang, Daniel M. Czajkowsky, Yi Shen, Jielin Sun, Chunhai Fan, Jun Hu, and Zhifeng Shao

Citation: [Applied Physics Letters](#) **102**, 073110 (2013); doi: 10.1063/1.4793205

View online: <http://dx.doi.org/10.1063/1.4793205>

View Table of Contents: <http://scitation.aip.org/content/aip/journal/apl/102/7?ver=pdfcov>

Published by the [AIP Publishing](#)

The advertisement features a photograph of the Model PS-100 probe station, a complex piece of scientific equipment with various mechanical components and a probe. The background is a gradient of blue. Text on the left includes 'NEW' in orange, 'Model PS-100' in large blue font, and 'Preconfigured Tabletop Probe Station' in smaller blue font. On the right, the 'Lake Shore CRYOTRONICS' logo is shown, with 'Lake Shore' in white and 'CRYOTRONICS' in blue. Below the logo, the tagline 'An affordable solution for a wide range of research' is written in white italicized font.

Bias controlled capacitive driven cantilever oscillation for high resolution dynamic force microscopy

Jinjin Zhang,¹ Daniel M. Czajkowsky,^{2,a)} Yi Shen,² Jieli Sun,² Chunhai Fan,¹ Jun Hu,¹ and Zhifeng Shao^{2,3,b)}

¹Physical Biology Laboratory, Shanghai Institute of Applied Physics, Chinese Academy of Sciences, Shanghai 201800, China

²Key Laboratory of Systems Biomedicine, Shanghai Jiao Tong University, Shanghai 200240, China

³School of Biomedical Engineering, Shanghai Jiao Tong University, Shanghai 200240, China

(Received 14 January 2013; accepted 7 February 2013; published online 21 February 2013)

Well controlled cantilever oscillations are essential for precise measurements in dynamic force microscopy and spectroscopy, especially in demanding conditions such as under solution or at high frequencies. Here, we show that, with a capacitive driving system, an externally introduced DC-bias significantly increases the driving efficiency in solution and in air, as well as at high resonant frequencies, in agreement with theoretical predictions. This DC-voltage dependence not only improves the robustness of the method but also offers the possibility for precise amplitude control. The simplicity of this design further reinforces its potential for widespread implementation in dynamic force microscopy. © 2013 American Institute of Physics.

[<http://dx.doi.org/10.1063/1.4793205>]

Advances in cantilever-based microelectromechanical systems (MEMS) have relied upon methodologies to produce stable, well controlled oscillations and resonances of the free-standing lever in order to sensitively detect small and localized interactions.^{1–9} For example, dynamic force microscopy utilizes changes in amplitude or in resonance frequency of tip-attached cantilevers to reveal sub-nanometer surface topographic features of individual molecules and surfaces,^{10–13} and micromechanical cantilever-based biosensors can detect down to femtomolar quantities of biosamples from minute changes to the resonance frequency.²

Presently, the most common method to drive the cantilever oscillation is by indirect mechanical agitation using a piezoelectric actuator embedded in the cantilever holder.^{14–16} While this is technically straightforward to implement, there are recognized complications with this excitation method in low Q environments as well as in the rapidly developing applications of high frequency (MHz) cantilevers.^{17–21} An example of the former is operation in aqueous solutions, where hydrodynamic coupling of the cantilever holder with the liquid often produces multiple spurious resonances, which can profoundly affect application.^{22,23} Similarly, off-resonance modes generated by the piezo-driven holder make more significant contributions to the cantilever oscillation when the driving frequency exceeds 1 MHz even in high Q environments.¹⁹ To overcome these difficulties, several direct coupling techniques have been developed.^{24–32} Directly driving magnetized cantilevers with an AC magnetic field generated by a coil has been shown to be effective for operation in liquids,²⁵ although this mechanism requires special instrumentation (including ferromagnetic-coated cantilevers) and the high impedance of the coil hampers its application at higher frequencies.^{30,31} Photothermal excitation methods can

also be used to directly drive the cantilever,³² but these methods require complicated optical components.³³ More sophisticated microfabrication technology has also enabled the production of actuators or capacitors to be grown directly on the cantilever for direct driving capability,³⁴ including a recent implementation specifically for high frequency applications.³⁵

Of particular interest in this regard, Umeda *et al.*³⁶ recently demonstrated that a conductive cantilever could be driven into resonance by directly coupling an AC field at the resonant frequency through an electrolyte solution. This simple, elegant mechanism is relatively easy to implement and should have a great potential for widespread use if it could be shown effective in many other environments, such as air or vacuum. However, the coupling efficiency demonstrated in this work is limited and the observed frequency dependence appears counterintuitive. Although the authors suggested surface stress as the underlying mechanism (at least with soft cantilevers), a closer examination of the system clearly suggests a capacitor-like driving mechanism: the metal coated cantilever and the distantly placed electrode form a simple capacitor-like assembly between which an external voltage is applied (Fig. 1). The capacitive force acting directly on the cantilever would thus be described by the well known relation³⁷

$$F_{drive} = \frac{1}{2} \frac{dC}{dZ} V^2, \quad (1)$$

where C , Z , and V are the capacitance, distance, and the electric potential between the cantilever and the other electrode, respectively. With the voltage given by $V = V_0 + V_{AC} \sin(2\pi ft)$ and treating the cantilever as a simple oscillator, the equation of cantilever motion is given by

$$Z = A_1(f) \sin(2\pi ft + \varphi_1) + A_2(2f) \sin(4\pi ft + \varphi_2), \quad (2)$$

where

^{a)}Electronic mail: daniel@sinap.ac.cn.

^{b)}Electronic mail: zfsao@sjtu.edu.cn.

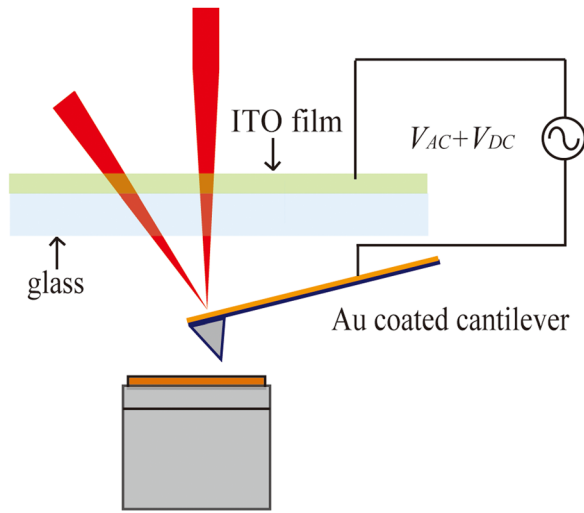


FIG. 1. Schematic diagram of the experimental setup for the capacitive force-driven FM-AFM. The backside of the cantilever is coated with gold and the top surface of the subtending glass is coated with transparent ITO. The AC- and DC-voltage signals are applied between the cantilever and the ITO coating to induce electrostatic interactions, which directly drive the cantilever.

$$A_1(f) = \frac{dC}{dZ} \frac{V_0 V_{AC}}{m} \frac{1}{4\pi^2 [(f_0^2 - f^2)^2 + f_0^2 f^2 / Q^2]^{\frac{1}{2}}}, \quad (3)$$

$$A_2(2f) = \frac{1}{4} \frac{dC}{dZ} \frac{V_{AC}^2}{m} \frac{1}{4\pi^2 [(f_0^2 - 4f^2)^2 + 4f_0^2 f^2 / Q^2]^{\frac{1}{2}}}, \quad (4)$$

and m , f_0 , and Q are the mass, resonance frequency, and quality factor of the free cantilever, respectively. We note that this V_0 should contain two components

$$V_0 = V_{DC} - V_{CPD}, \quad (5)$$

where V_{DC} is the applied DC-voltage and V_{CPD} is the contact potential difference as well established by Kelvin probe microscopy.³⁸ When the coating materials on the cantilever and the distant electrode are different, $V_{CPD} \neq 0$.³⁹

Hence, in this model, for nonzero V_0 , the cantilever can be driven into its natural resonance either at the resonance frequency ($f=f_0$), with amplitude given by A_1 , or at one half of the resonant frequency ($f=1/2f_0$), with amplitude given by A_2 . More generally, when driven at an arbitrary frequency, the cantilever oscillation should contain two components, with frequencies f and $2f$, although the amplitude of either component could be exceedingly small when driven at far off resonance. It is important to note that when $V_0=0$, only the A_2 term is nonzero, and so the cantilever resonance can only be excited by driving at $1/2f_0$. This is owing to the fact that regardless of the polarity, a nonzero potential between the two electrodes of a capacitor always leads to an attractive force. Since the applied V_{DC} was zero in Umeda *et al.*,³⁶ the observed resonance when driven at f_0 could be explained by a nonzero V_{CPD} , owing to the different materials used in the coating of the two electrodes.

To determine whether the above description is valid, we first investigated the cantilever response to various driving

frequencies using a home-built frequency modulation-atomic force microscope (FM-AFM) with a low noise deflection system⁴⁰ under ambient conditions (Fig. 1). In this setup, the cantilever oscillation is driven by the voltage applied (Function Waveform Generator, Agilent 33120A) between the gold-coated cantilever (Nanosensors, NCHAuD, $k=42$ N/m) and a transparent, metal coated (indium tin oxide, ITO) glass above the cantilever. Since the commonly cited work functions for gold and ITO are about 5.1 eV and 4.7 eV,^{41–43} respectively, $V_{CPD}=0.4$ V in this situation. During imaging, a FM detector (Nanosurf EasyPLL Plus) was used to generate the frequency shift signal for the feedback signal, and the sample position was controlled with a commercial controller (Nanoscope 3D, Bruker).

As shown in Fig. 2, with this setup, we indeed found that there are two peaks in the amplitude spectrum in air: there is a peak when the driving frequency is ~ 270 kHz, which is the resonant frequency (f_0) of this cantilever (as determined from the thermal oscillation (inset to Fig. 2)), and one when the driving frequency is $1/2f_0$ at ~ 135 kHz. Note that for both peaks, the actual oscillation of the cantilever is at the resonant frequency f_0 . The amplitude ratio between these peaks ($A_1/A_2 \sim 1.11$) is consistent with the expected ratio according to Eqs. (3) and (4) ($A_1/A_2 \sim 1.04$, for $V_{AC}=1.5$ V and $V_{CPD}=0.4$ V). The values of the quality factor, Q , obtained at each of these driving frequencies by fitting each peak to Eqs. (3) and (4), is also roughly the same (185 ± 2 at $f=f_0$ and 190 ± 1 at $f=1/2f_0$), as expected, providing additional confirmation of this theory.

Based on Eqs. (3) and (4), we also expect distinct dependencies on the applied AC and DC potentials for the amplitudes at the two driving frequencies. As shown in Figs. 3(a) and 3(b), we found that at $f=f_0$, there is a linear dependence of the amplitude on V_{AC} , whereas the amplitude first linearly decreases and then increases when V_{DC} varies from -1 V to 1 V. Both of these observations are in excellent agreement with Eq. (3). With the latter, the observed minimum at external $V_{DC}=+0.4$ V (Fig. 3(b)) is precisely the value predicted from the work function differences between ITO and Au (4.7 eV and 5.1 eV, respectively). The residual amplitude at $V_{DC}=+0.4$ V is the same as the intrinsic thermal amplitude without any external drive. At the $1/2f_0$

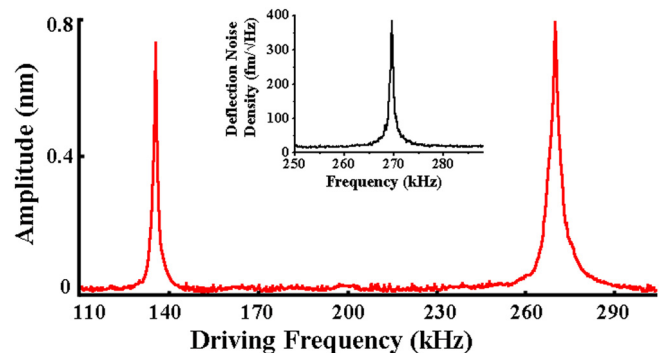


FIG. 2. The dependence of the amplitude on the driving frequency in air exhibits two peaks, one when the driving frequency is f_0 (~ 270 kHz) and the other when the driving frequency is $1/2f_0$ (~ 135 kHz), as predicted from the theory. The inset is the experimental spectra of the thermal noise motion of the cantilever in air.

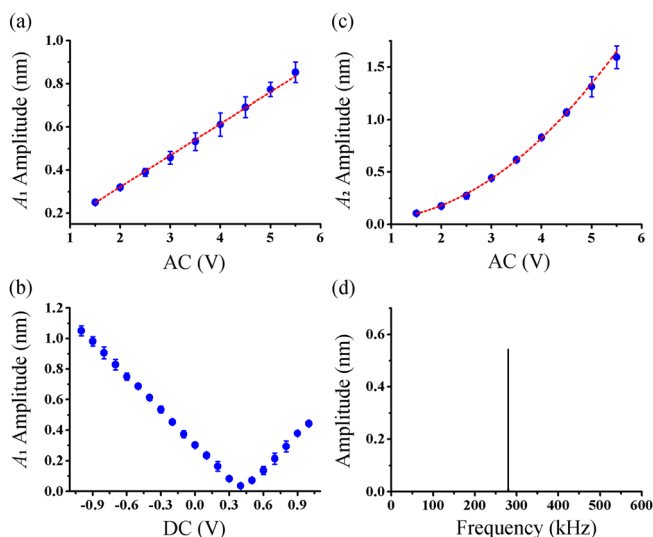


FIG. 3. Voltage dependencies of the measured amplitudes, A_1 and A_2 , in air, are consistent with the theory. (a) The oscillation amplitude of the cantilever at $f=f_0$ is linearly proportional (red line, $R^2=0.998$) to the amplitude of the AC driving voltage as predicted by Eq. (3). (b) The DC-voltage dependence of the amplitude at this same frequency is more complicated, first decreasing and then increasing with increasing voltage. This behavior however is consistent with Eq. (3), with the minimum value occurring at $V_{DC}=V_{CPD}$. (c) The oscillation amplitude at $f=1/2f_0$ is proportional to V_{AC}^2 (red line, $R^2=0.999$), as predicted by Eq. (4). (d) Fourier transform of the cantilever oscillation amplitude with driving frequency $f=f_0$ shows a single harmonic oscillation and the $2f_0$ component is negligible.

driving frequency, the resonant amplitude is proportional to V_{AC}^2 (Fig. 3(c)) and there is no DC-voltage dependence to the amplitude (data not shown), as expected from Eq. (4).

These experimental results thus demonstrate that the underlying driving mechanism of this setup is indeed consistent with a simple capacitor-like description. However, we should note that, according to this description, when the cantilever is driven at f_0 , there should be a $2f_0$ component as well (the A_2 term), which could excite higher harmonics or other resonance modes.^{44,45} When too large, these additional oscillatory modes could complicate the use of this method in certain applications. We have thus evaluated the significance of this potential complication in our setup by obtaining the Fourier transform of real-time recordings of the oscillation when driven at f_0 . As shown in Fig. 3(d), only a single harmonic oscillation was found and no other modes were significant (see below as well).

As the original report indicated that this driving mechanism does not depend on the DC-voltage in an electrolyte solution,³⁶ we further evaluated our model under these conditions. As observed in air, there are two peaks in the amplitude spectrum in aqueous solution (Fig. 4): one when the driving frequency is ~ 140 kHz, the resonance frequency in solution (as determined from the thermal spectrum, data not shown) and one at one half of the resonance frequency, ~ 70 kHz. Moreover, the measured amplitude ratio ($A_1/A_2 \sim 1.2$) is close to that expected from Eqs. (3) and (4) ($A_1/A_2 \sim 1.15$, with $V_{AC}=2$ V and $V_{DC}=1$ V), and the quality factors obtained at each frequency are also roughly the same (9.5 ± 0.5 , 8.9 ± 0.5 at f_0 and $1/2f_0$, respectively). Finally, the AC- and DC-voltage dependencies to the oscillation amplitude are also consistent with Eqs. (3) and (4) (Fig. 5).

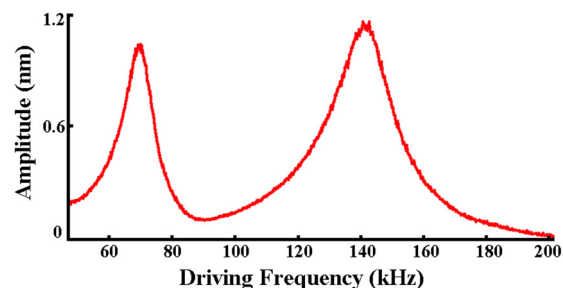


FIG. 4. The dependence of the amplitude on driving frequency exhibits two peaks at f_0 (~ 140 kHz) and $1/2f_0$ (~ 70 kHz) as predicted from the theory. Measurements were performed in 0.1 M KCl. For operation in solution, the ITO glass must be oriented such that the ITO film does not contact the solution (Fig. 1), which differs from the glass orientation described in the previous report (see Ref. 36).

It is worth pointing out that in these experiments, the subtending glass electrode must be oriented such that the conductive material is not in contact with aqueous solution (Fig. 1), which is opposite to that described in Umeda *et al.*³⁶ If both electrodes are in contact with solution, potentially detrimental electrochemical reactions or a large current between the electrodes can occur when an appreciable DC-voltage is applied.⁴⁶ In fact, when the ITO coating is in contact with the solution, even a small DC-voltage can lead to serious damage of the nm thick coating owing to the current flow.

In general, the amplitude in solution is expected to be greater than that in air for the same applied voltages, owing to the proportional dependence of the capacitance on the dielectric constant, which is ~ 80 times greater in water than in air. The dielectric constant decreases at high frequency, but not significantly until above ~ 1 GHz,⁴⁷ and so this change would not affect applications in the MHz range. Finally, it is important to note that in this low Q environment, the oscillation

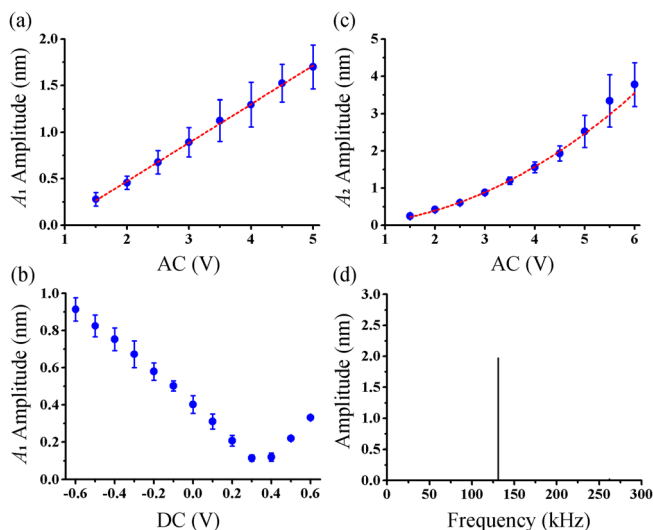


FIG. 5. Voltage dependencies of the measured amplitudes, A_1 and A_2 , in 0.1 M KCl are consistent with the theory. As found in air, the oscillation amplitude of the cantilever at $f=f_0$ is linearly proportional (red line, $R^2=0.998$) to the amplitude of the AC driving voltage (a), and exhibits a bimodal linear dependence on the DC-voltage as expected from Eq. (3). Also, the oscillation amplitude at $f=1/2f_0$ is proportional to V_{AC}^2 (c) (red line, $R^2=0.996$), as predicted by Eq. (4). (d) Fourier transform of the cantilever oscillation amplitude with driving frequency $f=f_0$ shows a simple harmonic oscillation.

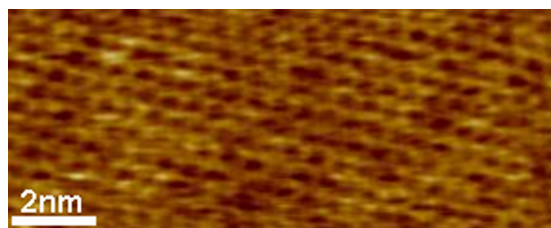


FIG. 6. High resolution image of mica obtained in 0.1 M KCl solution using the capacitive force driving method to drive the cantilever oscillation. To obtain this image, the amplitude was set at 0.5 nm, the $\delta f = 350$ Hz, and the scan rate was 6.1 Hz.

spectrum does not have the spurious peaks that are observed with the more common piezo-mechanical driven mechanism. Further, as noted above in air, the cantilever oscillation under this low Q condition can be essentially determined by the first resonance frequency, with no significant contribution of higher harmonics (Fig. 5(d)). Indeed, this driving mechanism was sufficiently stable to enable routine high resolution FM-AFM imaging in aqueous solution (Fig. 6).

To conclude, this simple capacitive force driving mechanism was found to effectively drive the cantilever both in air and in electrolyte solution, and the applied DC-voltage can significantly increase the efficiency of the AC drive at the resonant frequency, as it is routine to mix a small AC signal with a large DC offset electronically. As the oscillation amplitude is linearly dependent on the DC-voltage, this can thus be used to control the oscillation amplitude as a simple alternative to varying the AC drive, which not only allows its use in the feedback loop to control the amplitude but also for generating much higher amplitudes when required, simply by increasing the DC component to tens of volts. In addition, the small capacitance of this setup makes it well suited for higher frequency excitations. An advantage of this methodology is that it is simple to implement with commercially available cantilevers and requires only minimal changes to the instrumentation present in most labs. We believe that the DC-dependent mechanism described in the present work provides a simple alternative that will find wide use particularly in future MEMS applications utilizing cantilevers with MHz resonance frequencies for more rapid measurements in both AFM and biosensor investigations.

This work was financially supported by the National Basic Research Program (973 Program 2012CB932600, 2013CB932800, 2013CB932801, 2010CB529205), the National Natural Science Foundation (21073222, 91027020, 11074168, 21273148), and the Chinese Academy of Sciences (KJXC2-EW-N03).

¹M. Li, H. X. Tang, and M. L. Roukes, *Nat. Nanotechnol.* **2**, 114 (2007).

²J. L. Arlett, E. B. Myers, and M. L. Roukes, *Nat. Nanotechnol.* **6**, 203 (2011).

³N. V. Lavrik, M. J. Sepaniak, and P. G. Datskos, *Rev. Sci. Instrum.* **75**, 2229 (2004).

⁴L. M. Bellan, D. Wu, and R. S. Langer, *WIREs Nanomed. Nanobiotechnol.* **3**, 229 (2011).

⁵R. Lal, S. Ramachandran, and M. F. Arnsdorf, *AAPS J.* **12**, 716 (2010).

⁶C. Espenel, M. C. Giocondi, B. Seantier, P. Dosset, P. E. Milhiet, and C. L. Grimellec, *Ultramicroscopy* **108**, 1174 (2008).

⁷R. P. Richter and A. R. Brisson, *Biophys. J.* **88**, 3422 (2005).

⁸L. Xu, H. Bluhm, and M. Salmeron, *Surf. Sci.* **407**, 251 (1998).

⁹Q. Peng and H. Li, *Proc. Natl. Acad. Sci. U.S.A.* **105**, 1885 (2008).

¹⁰R. Garcia and R. Perez, *Surf. Sci. Rep.* **47**, 197 (2002).

¹¹Z. Shao, J. Mou, D. M. Czajkowsky, J. Yang, and J.-Y. Yuan, *Adv. Phys.* **45**, 1 (1996).

¹²D. M. Czajkowsky and Z. Shao, *J. Microsc.* **211**, 1 (2003).

¹³E. S. Andersen, M. Dong, M. M. Nielsen, K. Jahn, R. Subramani, W. Mamdouh, M. M. Golas, B. Sander, H. Stark, C. L. P. Oliveira, J. S. Pedersen, V. Birkedal, F. Besenbacher, K. V. Gothelf, and J. Kjems, *Nature* **459**, 73 (2009).

¹⁴Q. Zong, D. Innis, K. Kjoller, and V. B. Elings, *Surf. Sci. Lett.* **290**, L688 (1993).

¹⁵P. K. Hansma, J. P. Cleveland, M. Radmacher, D. A. Walters, P. E. Hillner, M. Bezanilla, M. Fritz, D. Vie, H. G. Hansma, C. B. Prater, J. Massie, L. Fukunaga, J. Gurley, and V. Elings, *Appl. Phys. Lett.* **64**, 1738 (1994).

¹⁶C. A. J. Putman, K. O. Van der Werf, B. G. De Groot, N. F. Van Hulst, and J. Greve, *Appl. Phys. Lett.* **64**, 2454 (1994).

¹⁷T. E. Schäffer, J. P. Cleveland, F. Ohnesorge, D. A. Walters, and P. K. Hansma, *J. Appl. Phys.* **80**, 3622 (1996).

¹⁸U. Rabe, S. Hirsenkorn, M. Reinstadtler, T. Sulzbach, C. Lehrer, and W. Arnold, *Nanotechnology* **18**, 044008 (2007).

¹⁹M. Shibata, H. Yamashita, T. Uchihashi, H. Kandori, and T. Ando, *Nat. Nanotechnol.* **5**, 208 (2010).

²⁰C. Leung, A. Bestembayeva, R. Thorogate, J. Stinson, A. Pyne, C. Marcovich, J. L. Yang, U. Drechsler, M. Despont, T. Jankowski, M. Tschöpe, and B. W. Hoogenboom, *Nano Lett.* **12**, 3846 (2012).

²¹I. Casuso, J. Khao, M. Chami, P. P. Gilloteaux, M. Husain, J. P. Duneau, H. Stahlberg, J. N. Sturgis, and S. Scheuring, *Nat. Nanotechnol.* **7**, 525 (2012).

²²H. J. Butt, P. Siedle, K. Seifert, K. Fendler, T. Seeger, E. Bamberg, A. L. Weisenhorn, K. Goldie, and A. Engel, *J. Microsc.* **169**, 75 (1993).

²³G. Y. Chen, R. J. Warmack, T. Thundat, D. P. Allison, and A. Huang, *Rev. Sci. Instrum.* **65**, 2532 (1994).

²⁴X. Xu and A. Raman, *J. Appl. Phys.* **102**, 034303 (2007).

²⁵W. H. Han, S. M. Lindsay, and T. W. Jing, *Appl. Phys. Lett.* **69**, 4111 (1996).

²⁶B. Rogers, D. York, N. Whisman, M. Jones, K. Murray, and J. D. Adams, *Rev. Sci. Instrum.* **73**, 3242 (2002).

²⁷A. Buguin, O. Du Roure, and P. Silberzan, *Appl. Phys. Lett.* **78**, 2982 (2001).

²⁸O. Enders, F. Korte and H.-A. Kolb, *Surf. Interface Anal.* **36**, 119 (2004).

²⁹G. E. Fantner, W. Schumann, R. J. Barbero, A. Deuschinger, V. Todorov, D. S. Gray, A. M. Belcher, I. W. Rangelow, and K. Youcef-Toumi, *Nanotechnology* **20**, 434003 (2009).

³⁰D. Ramos, J. Tamayo, J. Mertens, and M. Calleja, *J. Appl. Phys.* **99**, 124904 (2006).

³¹T. Fukuma, *Rev. Sci. Instrum.* **80**, 023707 (2009).

³²G. C. Ratcliff, D. A. Erie, and R. Superfine, *Appl. Phys. Lett.* **72**, 1911 (1998).

³³S. Nishida, D. Kobayashi, T. Sakurada, T. Nakazawa, Y. Hoshi, and Kawakatsu, *Rev. Sci. Instrum.* **79**, 123703 (2008).

³⁴J. Brugger, N. Blanc, Ph. Renaud, and N. F. de Rooij, *Sens. Actuators, A* **43**, 339 (1994).

³⁵K. A. Brown, B. H. Yang, and R. M. Westervelt, *Appl. Phys. Lett.* **100**, 053110 (2012).

³⁶K. I. Umeda, N. Oyabu, K. Kobayashi, Y. Hirata, K. Matsushige, and H. Yamada, *Appl. Phys. Express* **3**, 065205 (2010).

³⁷J. D. Jackson and R. F. Fox, *Classical Electrodynamics*, 3rd ed. (Wiley, New York, 1999).

³⁸M. Nonnenmacher, M. P. O'Boyle, and H. K. Wickramasinghe, *Appl. Phys. Lett.* **58**, 25 (1991).

³⁹M. Böhmisch, F. Burmeister, A. Rettenberger, J. Zimmermann, J. Boneberg, and P. Leiderer, *J. Phys. Chem. B* **101**, 10162 (1997).

⁴⁰T. Fukuma, M. Kimura, K. Kobayashi, K. Matsushige, and H. Yamada, *Rev. Sci. Instrum.* **76**, 053704 (2005).

⁴¹H. B. Michaelson, *J. Appl. Phys.* **48**, 4729 (1977).

⁴²Y. Zhou, J. W. Shim, C. Fuentes-Hernandez, A. Sharma, K. A. Knauer, A. J. Giordano, S. R. Marder, and B. Kippelen, *Phys. Chem. Chem. Phys.* **14**, 12014 (2012).

⁴³S. H. Kim, J. Jang, B. D. Chin, and J. Y. Lee, *Curr. Appl. Phys.* **8**, 475 (2008).

⁴⁴T. R. Rodríguez and R. García, *Appl. Phys. Lett.* **80**, 1646 (2002).

⁴⁵D. Kiracofe and A. Raman, *Phys. Rev. B* **86**, 205405 (2012).

⁴⁶R. N. Goyal, V. K. Gupta, M. Oyama, and N. Bachheti, *Electrochem. Commun.* **8**, 65 (2006).

⁴⁷Y. Z. Wei and S. Sridhar, *J. Chem. Phys.* **92**, 923 (1990).